This article was published in

J. Sainio, M. Aronniemi, O. Pakarinen, K. Kauraala, S. Airaksinen, O. Krause, J. Lahtinen, An XPS study of CrO$_x$ on a thin alumina film and in alumina supported catalysts, Applied Surface Science 252, 1076-1083 (2005).

An XPS study of CrO$_x$ on a thin alumina film and in alumina supported catalysts

J. Sainio [a,*], M. Aronniemi [a], O. Pakarinen [a], K. Kauraala [a], S. Airaksinen [b], O. Krause [b], J. Lahtinen [a]

[a] Laboratory of Physics, Helsinki University of Technology, P.O. Box 1100, FIN-02015 HUT, Finland
[b] Department of Chemical Technology, Helsinki University of Technology, FIN-02015 HUT, Finland

Abstract

We have investigated chromium layers evaporated onto a thin alumina film at room temperature. The oxidation and reduction behavior of this model catalyst was compared to atomic layer deposition (ALD) and impregnated alumina supported catalysts using X-ray photoelectron spectroscopy (XPS) with a detailed analysis method utilizing asymmetric peak shapes to represent both metallic and oxidic states. The ALD and impregnated catalysts were measured after calcination in air and after reduction with several gases at 850 K. Both catalysts show Cr^{3+} and Cr^{6+} species after calcination and mostly Cr^{3+} after reduction. The chromium layers deposited in vacuum show initially small partial oxidation due to the interaction with the oxygen terminated alumina film. These model catalysts can be oxidized in vacuum to Cr^{3+} species but not to higher oxidation states. The model catalysts were also subjected to calcination and reduction treatments after deposition in vacuum. Under these conditions the model systems exhibit similar oxidation/reduction behavior as the supported catalysts. Photoreduction of Cr^{6+} during the measurements was also studied and found to be very slow having a negligible effect on the results.
© 2005 Elsevier B.V. All rights reserved.

1. Introduction

Alumina supported chromium oxide catalysts are used in the petrochemical industry e.g. for dehydrogenation of alkanes to alkenes. XPS has extensively been utilized in the studies of these supported catalysts [1–3]. These studies have shown that alumina supported chromium catalysts exhibit two main oxidation states after calcination in air, Cr^{3+} and Cr^{6+}. The activity of the catalyst has generally been assigned to coordinatively unsaturated Cr^{3+} ions. Reduction of the catalysts in e.g. hydrogen leads mainly to Cr^{3+} species. Other chromium

* Corresponding author. Tel.: +358 9 4513130;
fax: +358 9 4513116.
E-mail address: jani.sainio@hut.fi (J. Sainio).

oxidation states have also been observed such as Cr^{2+} on silica [4] and Cr^{5+} on alumina under mild reductions [5].

The amount of information on the catalyst structure and reaction pathways obtainable from catalysts on porous supports is quite limited. Therefore, several studies have been performed on model catalysts created in ultra high vacuum (UHV) conditions [6–11]. The insulating nature of common support materials has led to the use of thin oxide films on metals, thus avoiding charging problems. The use of single crystal surfaces with a well-defined oxide structure allows the detailed study of the metal–oxide interface.

Most of the model catalyst work in the literature is concentrated on catalysts were the active species is metallic, often achieved by evaporation of the metal on the support in UHV. However, if the active species is an oxide, we face the additional challenge of controlling the oxidation state of the metal. An oxide model catalyst should exhibit the same oxidation and reduction properties as supported catalysts. This information is most easily obtained with XPS, since it is sensitive to the chemical state of surface atoms.

In this paper, we have studied the $Cr/Al_2O_3/NiAl(1\ 1\ 0)$ model system and compared the behavior of chromium on the surface to alumina supported Cr catalysts prepared by both impregnation and atomic layer deposition (ALD). In the ALD technique the precursor of the metal oxide is deposited on the support from the gas phase through saturating gas–solid reactions [2,12].

The model catalysts were prepared by evaporating Cr on a thin alumina film formed on a NiAl(110) single crystal sample. The thin and highly ordered alumina film is well suited to serve as a model substrate for catalyst studies, partially owing to its resemblance with the structure of γ-Al_2O_3. However, we are aware that the oxide layer is very thin and thus the metallic properties of the substrate can alter the oxide properties. It is also known that the surface does not contain OH groups that are thought to be important in the metal–oxide interaction taking place during e.g. impregnation. Other differences between our model system and supported catalysts come from the porosity of the support material. The purpose of this study was to compare oxidized and reduced model and supported catalysts to find out whether they exhibit similar behavior despite the above-mentioned differences.

In this work, we have made XPS measurements with the model catalyst and catalysts prepared by impregnation or ALD. The chromium oxidation state proportions have been determined quantitatively using a detailed analysis method utilizing reference spectra and asymmetric peak shapes. We observe that the catalysts show similar behavior in calcination and reduction, although the Cr^{6+} oxidation state was not formed on the model catalyst in vacuum conditions.

2. Experimental

The experiments reported in this paper were performed with two standard UHV systems with base pressures around 2×10^{-10} Torr.

The model catalyst construction was done in a chamber equipped with facilities for AES, XPS, TDS, LEED and metal evaporation. AES was measured utilizing a double pass cylindrical mirror analyzer (DPCMA) with an integral electron gun. Al $K\alpha$ radiation was used in the XPS experiments to avoid coincidence between the Ni Auger peaks caused by Mg $K\alpha$ irradiation and the Cr 2p emission. The binding energy scale was calibrated using the Ni $2p_{3/2}$ and Al $2p_{3/2}$ peaks of NiAl at 853.3 eV and 72.7 eV, respectively [13,14]. Cr 2p, Al 2p and O 1s XP spectra were measured from all samples.

The supported catalysts were measured in another chamber equipped with a SSX-100 ESCA spectrometer with facilities enabling XPS, ion sputtering and gas treatments in a separate reactor cell. The transfer to the reactor could be done without air exposure. After construction the model catalyst was transfered to this chamber and subjected to the same calcination/reduction treatments as the supported catalysts.

Calcinations were performed with laboratory air at 850 K for 30 min. Reductions of the supported catalysts were carried out with four gas mixtures: 5% H_2 in N_2, 10% CH_4 in Ar, 5% CO in N_2 and 10% *n*-butane in Ar. The model catalyst was reduced only with 5% H_2 in N_2. The gas flow through the reactor during treatments was approximately three liters per hour. The gas pressure in the reactor during reductions was above 1 atm to avoid possible air leakage into the reactor.

Al Kα radiation was used in the XPS experiments. A flood gun was used during XPS measurements to avoid charging problems caused by the insulating support. All binding energies of the supported samples were referenced to the alumina Al 2p peak at 74.0 eV. Cr 2p, Al 2p and O 1s XP spectra were measured from all samples.

2.1. Cr/Al₂O₃/NiAl(1 1 0)

Cleaning of the NiAl(1 1 0) sample was performed using Ar^+ ion sputtering for 60 min at room temperature followed by sputtering at 700 K for 30 min. Subsequent annealing at 1150 K for 45–60 min gave a sharp (1×1) LEED pattern. The cleanliness of the NiAl sample was measured using AES.

Formation of the 5 Å thick, well-ordered alumina film was performed by exposing the clean and annealed NiAl(1 1 0) sample to 3600 L $(1 L = 10^{-6}$ Torr s) O_2 at 550 K followed by annealing for 3 min at 1150 K. More information on this procedure has been given elsewhere [11,15–19]. The previously reported LEED pattern of the ordered alumina film [16] was used to confirm the correct surface structure.

Cr/Al₂O₃ model systems were prepared by thermal evaporation of chromium onto the Al₂O₃/NiAl(1 1 0) surface. The flux was evaluated to be $(3.4 \pm 0.2) \times 10^{12}$ Cr/cm² s. One coverage, corresponding to an evaporation time of 400 s, was used for comparison with supported catalysts. The topmost oxygen layer of the alumina film has an atomic density of 1.27×10^{15} at./cm²[16]. Using this as a value for a monolayer (ML) the chromium coverage would be 1.1 ML. Chromium oxide was formed by exposure to O_2 at 5×10^{-8} Torr for 400 s.

2.2. Cr/porous alumina

The chromia/alumina samples were prepared on AKZO 000-1.5E γ-alumina support calcined with air at 873 K for 16 h. The surface area of the support was 195 m²/g. The impregnated catalyst was prepared from $Cr(NO_3)_3 \cdot 9H_2O$ (Aldrich, 99%). After the impregnation the sample was stored overnight at room temperature, dried at 393 K for 4 h, and calcined with air at 873 K for 4 h. The ALD catalyst was prepared in a flow-type ALD reactor. The chromia precursor, chromium(III) acetylacetonate, $Cr(acac)_3$ (Riedel-de Haën, 99%), was vaporised and directed through the support bed held at 473 K. After the $Cr(acac)_3$ chemisorption, excess precursor was flushed from the reactor with nitrogen and the acac ligands were removed by air at 793 K. The chemisorption-ligand removal cycles were repeated 12 times. Thereafter, the catalyst was calcined with air at 873 K for 4 h.

The total chromium contents of the impregnated and ALD samples were 11 and 13.5 wt.% (AAS), or 6.5 and 8.0 Cr/nm², respectively. The Cr^{6+} content was according to UV–vis 3.2 wt.% for the impregnated sample and 2.9 wt.% for the ALD sample. Thus, the Cr^{6+}/Cr^{3+} ratios were 0.41 and 0.27, respectively. X-ray diffraction measurements indicated that the ALD sample did not contain any crystalline Cr_2O_3 species whereas the impregnated sample did.

2.3. XPS data analysis

Information on the chemical state of chromium ions was extracted from the 2p region of the XP spectrum. Curve fitting was used to resolve the overlapping peaks corresponding to different chemical states. Both metallic and oxidic states were represented with a mixed Gaussian–Lorentzian product function with a constant-exponential tail [20,21]. Reference spectra were recorded for metallic chromium (foil sample) and for the Cr^{3+} state (Cr_2O_3 powder sample), and the parameter values obtained from the these fits were used later in the analysis of the catalyst sample spectra. No reference sample was measured for the Cr^{6+} state; instead, the parameters were allowed to vary when fitting the first analyzed spectrum (Fig. 4) and then fixed to these values for the rest of the spectra.

Fig. 1 shows the 2p regions of the reference spectra of metallic and trivalent chromium. The spectrum of metallic chromium is fitted with two asymmetric peaks corresponding to the $2p_{1/2}$ and $2p_{3/2}$ states and a broad plasmon feature. The asymmetric lineshape results from the continuum of possible final states caused by interactions between conduction electrons and the core hole [22]. For the Cr^{3+} state, no plasmon was observed but the peaks for the two shake-up satellites need to be included in the fit. Also in the case of the oxidic state the lineshape is asymmetric. This is
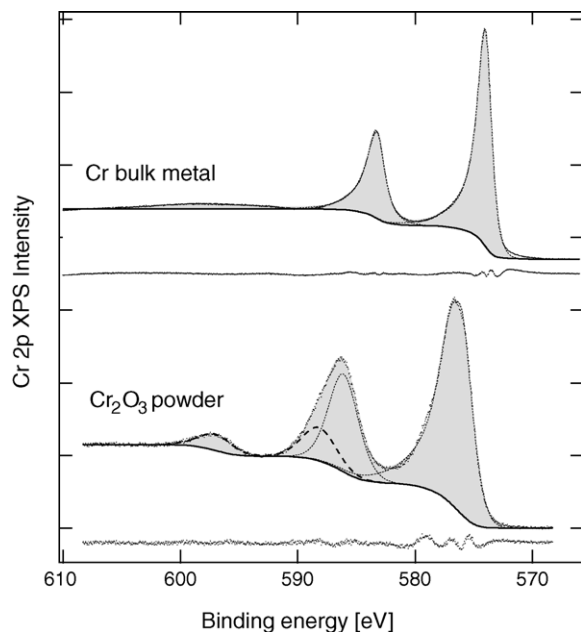
Fig. 1. Measured reference spectra for metallic chromium and Cr^{3+} with the fitted asymmetric doublets after Shirley background subtraction. Difference spectra are shown below the corresponding spectrum. The gray color represents the area under the fitted curve. The shake-up satellites of Cr^{3+} are drawn with a dashed line.
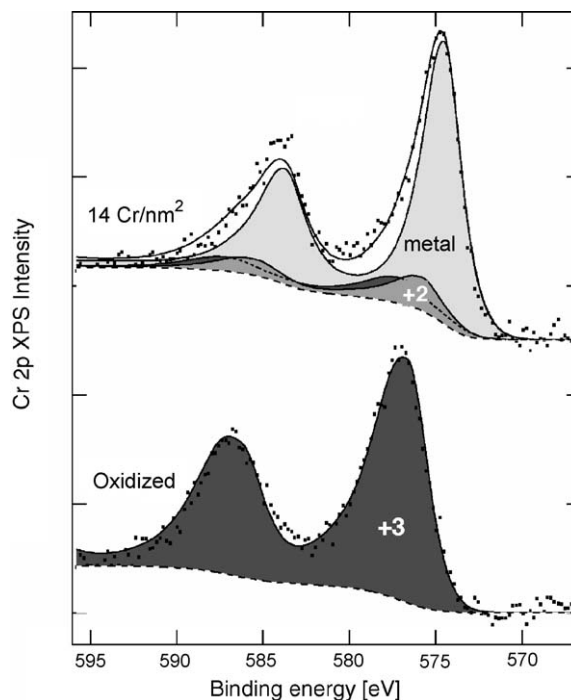

Fig. 2. Model catalyst with 14 Cr/nm^2 deposited at room temperature and oxidized with 20 L O_2. The oxidation states are indicated in the figure. Binding energy differences for all species were kept within ± 0.2 eV from reported values [11].

due to the multiplet splitting effect caused by unpaired 3d electrons [23].

Shirley background [24] was subtracted from each spectrum before the peak fitting. In order to prevent the background curve from exceeding the measured intensity, it was evaluated in two pieces. Details and the related errors of the spectrum analysis and background subtraction are considered in Ref. [21]. In particular, it has been shown that in the case of chromium oxide, the result of the chemical state quantification does not change significantly if the traditional Shirley background is replaced with the more physical Tougaard background. Using an asymmetric lineshape for the oxide states has instead been found to be essential.

3. Results

3.1. Model catalysts

When chromium was deposited onto the thin alumina film at room temperature mainly metallic

chromium, but also small amounts of oxidized chromium, was found on the surface. The accuracy of XPS in this case is not sufficient to clearly resolve the oxidation state distribution, but two more components corresponding to Cr^{3+} and Cr^{2+} had to be introduced to obtain a good fit. Fig. 2 shows Cr 2p XP spectra after deposition of 14 Cr/nm^2 at room temperature.

When oxidation of the chromium overlayers was performed using an O_2 exposure of 20 L ($1L = 10^{-6}$ Torr s), the Cr clusters formed at room temperature deposition could be totally oxidized to Cr^{3+} for all studied coverages as can be seen in Fig. 2 for 14 Cr/nm^2. The spectrum corresponds to Cr^{3+}.

The oxidized chromium layers could be reduced by heating the sample to 700 K for a few minutes. The resulting oxidation state distribution after reduction was similar to that after evaporation.

After the thermal reduction of room temperature grown chromium oxide, the aluminum oxide component in the Al 2p spectrum was found to increase.
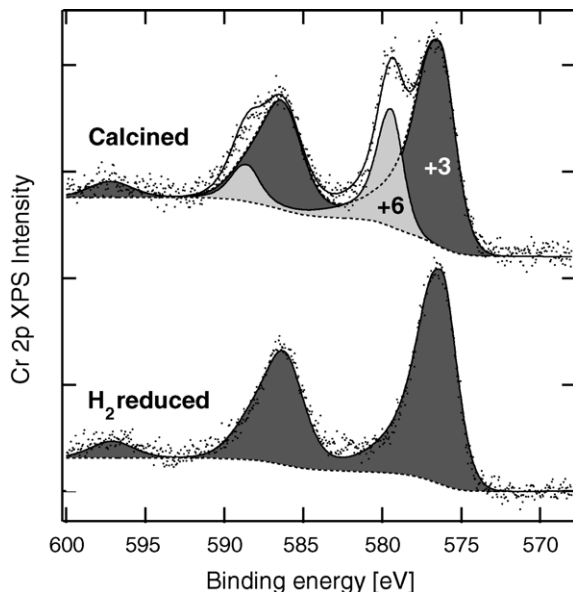
Fig. 3. Model catalyst with 14 Cr/nm^2 after calcination in air and after subsequent reduction in hydrogen.

Fig. 4. ALD catalyst after calcination in air and after subsequent reduction in hydrogen.

Thermal desorption experiments confirmed that oxygen was not desorbed during heating. This was interpreted as thickening of the alumina film. It was confirmed that at elevated temperatures with oxygen present, chromium oxide acts as a catalyst promoting the growth of the alumina film. Chromium oxide is able to dissociate oxygen and atomic oxygen can then react with bulk aluminum creating more aluminum oxide. This same effect has also been observed for other transition metals on Al_2O_3/NiAl(1 1 0), such as palladium and vanadium [9,25].

The chromium oxidation state 6+ could not be reached by any oxidation treatment in UHV conditions. Exposure of the model catalyst to air led to similar oxidation to Cr^{3+} as in vacuum. However, after calcination in air Cr^{6+} was also found on the model catalyst.

Fig. 3 shows the Cr 2p XP spectra of the model catalyst after calcination in air and after subsequent reduction with hydrogen. The component corresponding to Cr^{6+} is clearly visible in the spectra after calcination. H_2 treatment leads to complete reduction of the model catalyst back to Cr^{3+} species, but not to lower oxidation states.

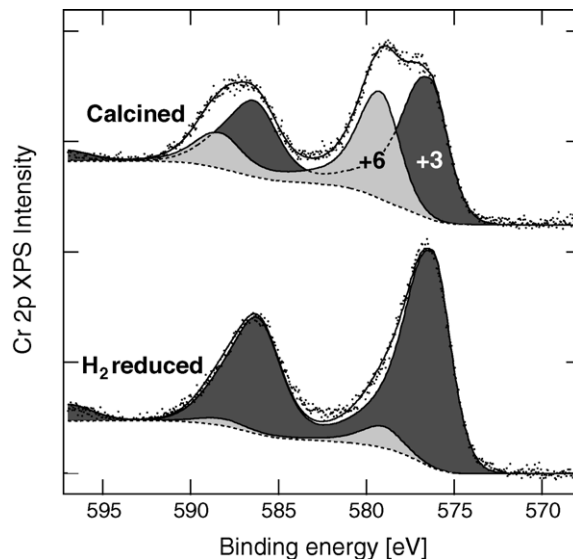The calcination treatment caused significant thickening of the alumina film. Evaluation of the Cr^{6+}

proportion in repeated calcination/reduction treatments was not therefore considered reliable and only values from the first treatments have been considered.

3.2. Supported catalysts

The changes in the oxidation states of the supported Cr catalysts were characterized with ESCA. All samples were calcined at 850 K in undried air prior to other treatments to achieve an even oxidation state distribution throughout the sample. The impregnated and ALD prepared catalysts were found to behave quite similarly in oxidation/reduction treatments. Fig. 4 shows a typical Cr 2p XP spectrum for a calcined supported catalyst with the two components, Cr^{3+} and Cr^{6+}. The amount of Cr^{6+} after calcination varied and was somewhat smaller for impregnated catalysts than ALD catalysts.

The supported Cr catalysts were reduced in several gases: H_2, CO, CH_4 and *n*-butane. After the reduction mainly Cr^{3+} species were found on the surface as shown in Fig. 4 for the ALD catalyst. The amount of Cr^{6+} of all chromium after reduction in any of the gases used was less than 10%. Signals that could be attributed to Cr^{2+}, Cr^{4+} or Cr^{5+} were not found after any treatments, indicating that their concentration was

Table 1
Proportion of Cr^{6+} of all chromium for different catalysts after calcination and reduction according to XPS

Catalyst	Calcined (%)	Reduced (%)
ALD	30–41	< 10
Impregnated	20–31	< 10
Model	19	< 5

The model catalyst treatments correspond to Fig. 3. The estimated error for an individual amount is ±2% units.

Fig. 5. The fraction of Cr^{6+} of all chromium as a function of XPS measurement time. The error of the slope is derived from a weighted least square fit.

clearly less than 5%. This was true also for the impregnated catalyst. Table 1 summarizes the oxidation state proportions for the three different type of catalysts.

The two supported catalysts differ from each other in the dispersion of the catalyst material. Kytökivi et al. [2] found that ALD results in practically atomic dispersion, being always better than with any impregnation method. The deposition of Cr on the model support is also likely to give poorer dispersion than ALD as long as the cluster size is fairly large and the growth mode is close to Volmer-Weber like 3D growth. Volmer-Weber growth has been observed for almost all transition metals on Al_2O_3/NiAl(1 1 0), see e.g. Refs. [25,26]. As for the cluster size, clusters of 20–30 Å in diameter have been observed at monolayer range coverage e.g. for vanadium [25]. Our preliminary AFM measurements of Cr on the model support indicate cluster sizes above this at a similar coverage.

The differences in dispersion between the catalysts did not seem to affect the general oxidation state behavior following different treatments. However, the slightly higher amount of Cr^{6+} observed on the ALD catalyst after oxidation could be due to better dispersion.

3.3. Photoreduction

It has previously been observed that the photoelectric process used in XPS can reduce the active metal [5]. In chromium catalysts it has been suggested that the measurement itself reduces Cr^{6+} to Cr^{4+} or Cr^{3+}[27], and therefore the observed fraction of Cr^{6+} after an extended measurement would be too small. The reduction has also been suggested to occur only if hydrocarbons are adsorbed onto the sample e.g. during rough pumping.
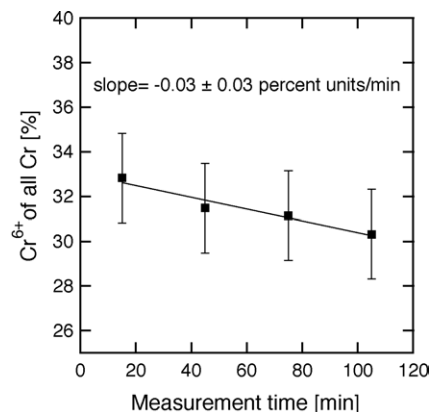
Photoreduction was studied with a calcined ALD catalyst to find out how it affects the observed oxidation state distribution. Consecutive measurements were carried out, each of which lasted 15 min. Fig. 5 shows the fraction of Cr^{6+} of all chromium as a function of cumulative measurement time. The points represent the fraction observed in the peak fitting after each measurement and are therefore time averages of the amounts of Cr^{6+}.

The reducing tendency of the measurement is indeed observed in Fig. 5, but its magnitude is very small. All measurements of the Cr 2p region in this work lasted about 15 min which would correspond to a reduction of 0.4%. This value is insignificant for our interpretation of the oxidation state distribution. However, long measurement times could lead to underestimation of Cr^{6+}.

4. Discussion

The model catalyst was found to exhibit different oxidation states in vacuum than at atmospheric pressures. During chromium growth small amounts of Cr^{3+} and Cr^{2+} species are found on the surface obviously due to interaction with the oxygen terminated film. In our experiments the Cr^{2+} species found on the model catalyst was readily oxidized to Cr^{3+} even in low oxygen pressures. Oxidation in vacuum, however, did not proceed further than Cr^{3+}.

Cr^{2+} is found on silica supported catalysts, where it is the active species. This has generated speculation that the active species on alumina should also be Cr^{2+}, although no direct evidence of its existence has been reported. In our experiments Cr^{2+} was not seen on the alumina supported catalysts nor on the model catalyst when subjected to atmospheric conditions, which is in agreement with other spectroscopic studies [1,3].

After calcination in air Cr^{6+} species was present on all studied catalysts, although it was not found on the fresh model catalyst under UHV. The formation of Cr^{6+} is likely to be a thermally activated process, because it was not found on reduced catalysts even after long exposures to oxygen at room temperature. Other factors that might effect the formation of Cr^{6+} are OH groups and the support structure.

OH groups are not inherently present in vacuum, but are thought to be important in the catalytic reactions. Libuda et al. have studied an OH modified Al_2O_3/NiAl(1 1 0) system and found direct chemical interaction between the rhodium deposits and the hydroxyl groups on the surface [28]. The calcinations in the present work were performed in undried air where OH groups are certainly present and can have an effect on the oxidation states of chromium.

The flat structure of NiAl(1 1 0) based samples is also very different if compared with the supported catalysts, which are porous. The thin alumina film on the model catalyst is initially highly ordered and flat. After calcination of the model catalyst, a significant increase in the thickness of the aluminum oxide film was observed, which was evaluated from the XPS intensities to be at least 30 Å. The surface ordering is also lost and new sites for chromium with different oxidation states could have been created.

Reduction of calcined samples led mainly to Cr^{3+} species with small amounts of Cr^{6+} left on the surface of supported catalysts. Since the samples exhibit similar qualitative behavior in oxidation and reduction, it should be possible to use the model catalyst to study e.g. the mechanism of alkane dehydrogenation.

5. Conclusions

We have investigated chromium catalysts and compared the oxidation/reduction behavior of two supported catalysts to a model catalyst created in ultra high vacuum using X-ray photoelectron spectroscopy (XPS).

The growth of Cr on the Al_2O_3/NiAl(1 1 0) model system was investigated at room temperature. The model catalyst showed partial initial oxidation of chromium on the oxygen terminated alumina film. Oxidation of the model system grown at 300 K led to Cr^{3+} species. The model catalyst could be reduced by heating and this results in a similar oxidation state distribution as after evaporation. This reduction process was found to increase the alumina film thickness by oxygen diffusion through the chromium film.

When the model catalyst was subjected to calcination in air flow, Cr^{6+} was also found on the catalyst. The calcination process causes severe thickening of the alumina film. The calcined catalyst could be reduced with hydrogen back to Cr^{3+}.

ALD and impregnated catalysts both showed oxidation states Cr^{3+} and Cr^{6+} after calcination. The reduction process removed most of the Cr^{6+} species from the catalyst surfaces and was independent of the reducing gas used. Photoreduction of Cr^{6+} during the measurements was found to be negligible.

The Cr/Al_2O_3/NiAl(1 1 0) model system was found to behave in a similar way in oxidation and reduction as alumina supported catalysts if subjected to atmospheric conditions. This would imply that the model system is indeed a relevant one even though the structures of the catalyst support materials differ greatly.

References

[1] F. Cavani, M. Koutyrev, F. Trifiró, A. Bartolini, D. Ghisletti, R. Iezzi, A. Santucci, G. Del Piero, J. Catal. 158 (1996) 236.
[2] A. Kytökivi, J.-P. Jacobs, A. Hakuli, J. Meriläinen, H.H. Brongersma, J. Catal. 162 (1996) 190.
[3] W. Grünert, E.S. Shpiro, R. Feldhaus, K. Anders, G.V. Antoshin, K.M. Minachev, J. Catal. 100 (1986) 138.
[4] A.B. Gaspar, J.L.F. Brito, L.C. Dieguez, J. Mol. Catal. A 203 (2003) 251.
[5] Y. Okamoto, M. Fujii, T. Imanaka, S. Teranishi, Bull. Chem. Soc. Jpn. 49 (4) (1976) 859.
[6] V. Nehasil, S. Zafeiratos, S. Ladas, V. Matolín, Surf. Sci. 433–435 (1999) 215.
[7] M. Bäumer, M. Frank, M. Heemeier, R. Kühnemuth, S. Stempel, H.-J. Freund, Surf. Sci. 454–456 (2000) 957.

[8] G. Rupprechter, H. Unterhalt, M. Morkel, P. Galletto, L. Hu, H.-J. Freund, Surf. Sci. 502–503 (2002) 109.

[9] S. Shaikhutdinov, M. Heemeier, J. Hoffmann, I. Meusel, B. Richter, M. Bäumer, H. Kuhlenbeck, J. Libuda, H.-J. Freund, R. Oldman, S.D. Jackson, C. Konvicka, M. Schmid, P. Varga, Surf. Sci. 501 (2002) 270.

[10] H.-J. Freund, Surf. Sci. 500 (2002) 271.

[11] M. Eriksson, J. Sainio, J. Lahtinen, J. Chem. Phys. 116 (2002) 3870.

[12] S.M.K. Airaksinen, A.O.I. Krause, J. Sainio, J. Lahtinen, K.-J. Chao, M.O. Guerrero-Peréz, M.A. Bañares, Phys. Chem. Chem. Phys. 5 (2003) 4371.

[13] S.-C. Lui, J.W. Davenport, E.W. Plummer, D.M. Zehner, G.W. Fernando, Phys. Rev. B 42 (1990) 1582.

[14] A. Stierle, C. Tieg, H. Dosch, V. Formoso, E. Lundgren, J.N. Andersen, L. Köhler, G. Kresse, Surf. Sci. 529 (2003) L263.

[15] H. Isern, G.R. Castro, Surf. Sci. 211–212 (1989) 865.

[16] R.M. Jaeger, H. Kuhlenbeck, H.-J. Freund, M. Wuttig, W. Hoffman, R. Franchy, H. Ibach, Surf. Sci. 259 (1991) 235.

[17] J. Libuda, F. Winkelmann, M. Bäumer, H.-J. Freund, T. Bertrams, H. Neddermeyer, K. Müller, Surf. Sci. 318 (1994) 61.

[18] S. Andersson, P.A. Brühwiler, A. Sandell, M. Frank, J. Libuda, A. Giertz, B. Brena, A.J. Maxwell, M. Bäumer, H.-J. Freund, N. Mårtensson, Surf. Sci. 442 (1999) 964.

[19] M. Klimenkov, S. Nepijko, H. Kuhlenbeck, H.-J. Freund, Surf. Sci. 385 (1997) 66.

[20] P.M.A. Sherwood, Data analysis in XPS and AES, in: D. Briggs, M.P. Seah (Eds.), Practical Surface Analysis, second ed. Auger and X-ray Photoelectron Spectroscopy, Vol. 1, John Wiley & Sons, Inc., 1990, pp. 555–586.

[21] M. Aronniemi, J. Sainio, J. Lahtinen, Surf. Sci. 578 (2005) 108.

[22] S. Doniach, M. Šunjić, J. Phys. C 3 (1970) 285.

[23] R.P. Gupta, S.K. Sen, Phys. Rev. B 12 (1975) 15.

[24] D.A. Shirley, Phys. Rev. B 5 (1972) 4709.

[25] M. Bäumer, J. Biener, R.J. Madix, Surf. Sci. 432 (1999) 189.

[26] J. Sainio, M. Eriksson, J. Lahtinen, Surf. Sci. 532–535 (2003) 396.

[27] S.V. Kagwade, C.R. Clayton, G.P. Halada, Surf. Interface Anal. 31 (2001) 442.

[28] J. Libuda, M. Frank, A. Sandell, S. Andersson, P.A. Brühwiler, M. Bäumer, N. Mårtensson, H.-J. Freund, Surf. Sci. 384 (1997) 106.